International Compressor Engineering Conference

School of Mechanical Engineering

2022

Comparison of Low-Cost Detection Methods for Liquid Refrigerant Flow at Compressor Inlet

Robin Langebach

Miroslav Andjelkovic

Tobias Pfliehinger

Franz Joseph Pal

Follow this and additional works at: https://docs.lib.purdue.edu/icec

Langebach, Robin; Andjelkovic, Miroslav; Pfliehinger, Tobias; and Pal, Franz Joseph, "Comparison of Low-Cost Detection Methods for Liquid Refrigerant Flow at Compressor Inlet" (2022). *International Compressor Engineering Conference.* Paper 2751.
https://docs.lib.purdue.edu/icec/2751

Comparison of Low-Cost Detection Methods for Liquid Refrigerant Flow at Compressor Inlet

Robin Langebach[1]*, Miroslav Andjelkovic[1],
Tobias Pfliehinger[1], Franz Joseph Pal[1]

[1]University of Applied Sciences, THE SCHAUFLER FOUNDATION Endowed Professorship for
Compressor Technology, Institute for Refrigeration, Air Conditioning and Environmental Technology
76133 Karlsruhe, Germany
Phone: +49 721 925 1853, Email: robin.langebach@h-ka.de.de

* Corresponding Author

ABSTRACT

Up to now, refrigerant compressors have been monitored in standard systems on the basis of continuous measurements of temperature, pressure, electrical variables and the oil level in the housing. Other measured variables are often not or only rarely taken into consideration due to comparatively high costs. These include, for example, mechanical vibrations or the vapor fraction in the suction line. In particular, the existence of liquid refrigerant in the suction line can be responsible for short-term damage as well as for continuous damage in the compressor over the long term. This includes liquid slugging as well as oil wash-out at important bearing points. Up to now, mainly capacitive sensors have been available for measuring the vapor fraction, which are only attractive in terms of price for very large refrigeration plants. In order to counter this situation in the future, three measurement methods for detecting liquid in the suction line of the compressor were investigated. These are optical detection by means of a camera and image recognition, optical detection of the light intensity when transilluminated by an LED, and the change in the natural frequency of a cantilever using a MEMS accelerometer. The results show that all three measurement methods are basically capable of reliably detecting of liquid refrigerant in the suction line at very low cost. The optical detection of the light intensity by transillumination with an LED has proven to be particularly suitable at best. In this case, the use of a standard inspection glass with few electronic components enables very good detection of the phase boundary and also filters out failure events, for example from machine oil passing the measurement section.

1. INTRODUCTION AND MOTIVATION

In almost all refrigeration and air conditioning systems as well as heat pumps, at least one refrigerant compressor performs its service - often inconspicuously and for years. According to industry projections, about 486 million compressors were introduced into the stationary market in 2021, market value approx. 42.4 billion dollars according to Felipe et al. (2019). That confirms energy-efficient refrigeration and air conditioning systems are a key to solving the climate crisis and can make a significant contribution to global energy savings. The compressors used span large capacity ranges, starting from a few watts of cooling capacity for small hermetic machines, e.g. for household refrigerators, to the megawatt range with large semi-hermetic or open machines, e.g. for building air conditioning or for logistics centers. The sales prices of compressors especially in the low capacity range are usually in the double-digit dollar range. However, the number of compressors on the market is particularly high, especially in the low-price segment. Although, digitization is noticeably picking up speed, it is being held back by strong cost pressures.
In order to achieve most reliable and energy-efficient systems, monitoring capabilities are necessary and still not sufficiently depleted. According to the state of the art, the oil level, temperatures, pressures and electrical parameters are usually recorded in monitoring modules for refrigerant compressors – in accordance to customers' requirements and willingness to spend extra monetary efforts. In combination with other measured data from the refrigeration system, these parameters already give a good perspective on operation and condition of the machine. However,

compressor failures can have many different causes – design shortcomings of the machine as well as by the refrigeration plant itself.

An unwanted consequence of inadequate refrigerant plant design is the intake of liquid refrigerant into the compressor during operation. Often, that goes completely undetected. Liquid refrigerant intake may result in two distinguished scenarios.

One is when liquid refrigerant moves – at least in quantities – straight through the compressor into the working chamber. Depending on the compressor type, this can result in damage to the valves and sealings, which often leads to short-term failure of the compressor. This scenario is - as far as possible - reproduced by the compressor manufacturers in tests and the machines are designed to be tolerant of it to a certain extent.

Second is when liquid refrigerant enters the compressor again and again for short time periods during operation. This can happen in transient operating conditions, when starting up the machine, or when the operating conditions change. This scenario does not immediately result in a failure of the machine. Rather, it can lead to longer-term, creeping damage due to undesirable side effects – such as washing out of the oil from bearing points.

With above mentioned monitoring parameters liquid refrigerant intake cannot be detected in adequate form. A way out can be vapor quality sensors that are already available on the market. The price level of those sensors is fairly high and hence application is only economical for large capacity machines. For low price applications in the mass market other sensor concepts need to be researched. Within this paper we investigate three sensor methods with the aim to provide at least a reliable trigger signal for liquid refrigerant passing through the suction line towards the compressor. The first sensor method (Method A) is about image processing, the second method (Method B) is about natural frequency analysis of a cantilever in the suction line flow, and the third method (Method C) is about transillumination of the suction line flow by an LED/Photodiode-array in the form of integral Optical Fluoroscopy.

In literature there are publications available which deal with these methods A-C in broader and narrower sense.

With respect to general evaluation of the liquid-vapor-content of a refrigerant flow Gardenghi et al. (2020) published a review paper with a discussion of various solutions to determine the vapor quality in refrigerant flows. Reviewed methods comprise mechanical, optical, ionizing radiation as well as electrical approaches.

With respect to Method A – Image Processing, Handoyo et al. (2018) studied the phase formation with laser and evaluated by an image processing software. Zhang et al. (2020) studied water and air motion in a horizontal glass tube using cameras and image processing library OpenCV. A camera system in combination with prism (multi-vision method) was used to create a 3D image based on two orthogonal perspectives. Ruiz et al. (2013) demonstrated the possibility of detecting pollution and making statements about emissions with the help of image processing library OpenCV. Felipe et al. (2019) presented a liquid volume detection method in an amber glass bottle, also by using OpenCV. Hence, the core statement of our literature study is the application of appropriate filters within the image processing software.

With respect to Method B – natural frequency analysis of a cantilever, Wang et al. (2016) published a new vibration probe sensor approach for measuring the mass flow rate in gas–solid two-phase flow. The used sensor is based on a polyvinylidene fluoride (PVDF) piezoelectric film. Average amplitude, standard deviation and spectral peak at the natural frequency of the probe were used as characteristic quantities to determine a relation between mass flow rate and air flow velocity. Xiao et al. (2019) proposed a slug model and piston-flow model for calculation of the flow forces acting on a tube bending. A model was provided to estimate flow forces depending on the flow regime within low deviation from measured values.

With respect to Method C – Integral Optical Fluoroscopy Revellin et al. (2006) described an optical setup with laser and photodiode in order to investigate vapor-liquid-flow in R134a pipes with small diameters. With the help of characterizing variables such as coalescence rates of bubbles, length distribution as well as mean velocity the authors could identify the flow regimes and transitions. Sarkodie et al. (2019) also investigated vapor-liquid-flow in a pipe with special focus to chemical industry. Within the study IR LEDs in combination with IR photodiodes were us at a transparent section in addition to a high-speed camera. The experiments aimed for determination of bubbles in the flow and coupled vibrations to the piping in order to continuously monitor the flow rate. In addition, Wu et al. (2019) used a similar setup by applying an infrared laser source and photodiode sensor array in order to accurately measure the gas void fraction in a two-phase CO_2 flow in transportation pipelines. Wu et al. (2019) concluded that for horizontal as well as for vertical pipelines this setup is reliable and effective in measuring the gas void fraction in the two-phase flow.

2. DESCRIPTION OF TEST RIG

The test rig used consists of a standard Tecumseh AET 4425 condensing unit with reciprocating compressor and uses the refrigerant R134a. The condensing unit has only a comparatively low refrigerating capacity of approx. 580 W at 5 °C. However, the primary objective is not to provide refrigerating capacity or to measure the same, but to provide liquid refrigerant in relevant quantities into the suction line to the compressor. The condensing unit was therefore equipped with a manually controlled expansion valve. After that, the refrigerant can either be fed directly to the evaporator via solenoid valves B or directly into the suction line in a bypass opened by solenoid valve A. In the suction line there are two sight glasses (A and B), to which the measuring methods for the qualitative determination of the liquid refrigerant have been attached.

For method A – image processing, the liquid passing through the sight glass can be directly observed with the camera. For method B – natural frequency analysis of a cantilever and method C – integral optical fluoroscopy, the first or second sight glass were adapted and are hence no longer can be used for visual observations. The distance between both sight glasses is approx. 30 cm. Hence, liquid passage may result in a certain time delay. Fig. 1 shows the test rig schematic for better understanding.

When solenoid valve A is opened and solenoid valve B is closed at the same time, liquid refrigerant enters the sight glasses directly bypassing the evaporator. If the manually controlled expansion valve is fully opened, a gush of liquid refrigerant can be transported through the sight glasses. A quantitative determination of the vapor quality is not possible with this arrangement. Rather, emphasis was placed on the targeted control of a qualitative liquid passage through both sight glasses. A suction gas accumulator was used to protect the compressor.
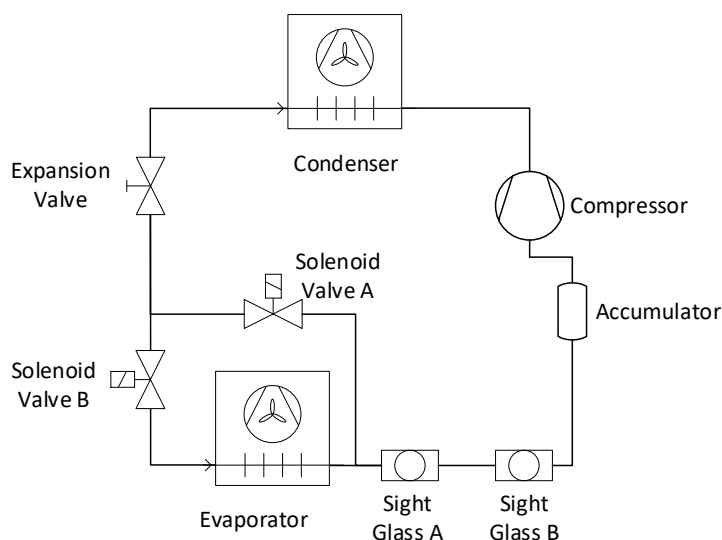

Figure 1: Test rig schematic

3. MEASUREMENTS WITH DIFFERENT APPROACHES

3.1 Method A – Image Processing

3.1.1 Approach and working principle
In this method, the approach is to use a camera to detect the vapor and liquid refrigerant in a sight glass via optical refraction and interface detection. Image processing software from OpenCV is used to transform the camera image into a binary black and white image in order to count black and white pixels. The main features of image processing are filter options like threshold to distinguish black and white zones. Figure 2 shows a schematic of the evaluation routine. The continuously running program performs the evaluation on a standard PC based on the camera data and image processing.

This is a non-invasive measurement method that does not require any modification of the plant except of the additional sight glass in the suction line. The camera setup used here costs about $50 and has a resolution of 1280 x 720 pixels with a frame rate of 60 fps.
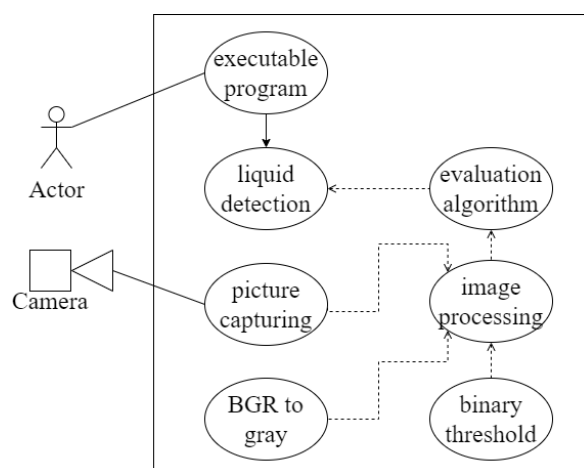

Figure 2: Schematic of the evaluation routine

3.1.2 Test setup

For the measurement, the camera is positioned at a distance of approx. 1.18 inch (3 cm) above the sight glass and aligned for best image qualtity of the camera.

Position and orientation are fixed at the beginning and not changed during the measurements. Figure 3 shows the experimental setup, which includes the test rig, the webcam and the evaluation PC. The evaluation liquid and vapor quality is maintained by a self-written C++ program, which accesses the camera image with OpenCV, performs the image by image processing as well as black/white analysis. A real time data acquisition and evaluation is possible.

The image processing routine uses an image section from the camera raw image to create a black and white image. Then a threshold filter (grayscale threshold value = 200) is used to adjust the contrast to maximize reflections from the bottom of the sight glass. By maximizing the reflection, the dynamics of the flow in the sight glass can be better displayed. Finally, the liquid refrigerant presence is evaluated based on the dynamic image using the binary image pixels. At the beginning of each measurement, a calibration must be carried out, during which the exact phase of the refrigerant must be known. It is therefore necessary to be able to ensure 100% vapor in the sight glass at the start of each measurement. Homogeneous illumination is very important for the method used here. To ensure this, the camera's built-in LED is used as an illumination source in this experiment.
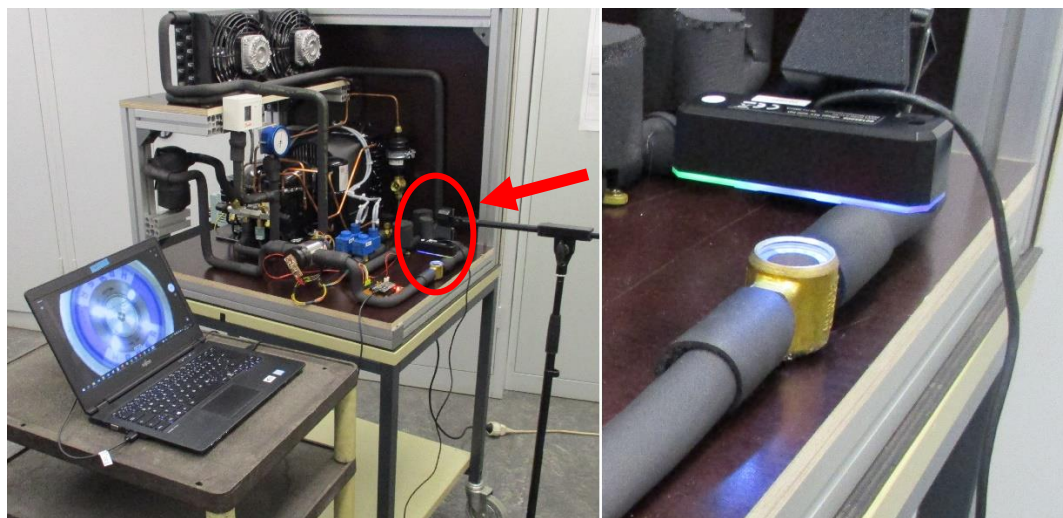
Figure 3: Camera test setup installed at test rig

3.1.3 Measurements and discussion

At the beginning of each measurement, an average value of the sum of binary pixels (black/white counting) was determined and over the period of 10 seconds as calibration procedure. During this, a mean value of 84833 white pixels was obtained as 100% vapor corresponding. Based on this, the upper and lower limits of ± 10% including a hysteresis were defined for the evaluation process.

In order to provoke liquid refrigerant running through the test section, the solenoid valves of Figure 1 are switched to activate the evaporator bypass. Figure 4 shows the sight glass processed with OpenCV at different times in color, grayscale and binary black/white mode. The sub-picture (A) shows the sight glass at the starting point where the sight glass is completely filled with vapor. In picture (B) the sight glass is shown when liquid refrigerant is entering in noticeable quantities. Comparing (A) and (B), the reflection of the sight glass bottom by the liquid refrigerant decreases due to refraction effects.

The discussed measurement was recorded over 80 seconds. The results as event evaluation are shown in of Figure 5 (top). After opening the solenoid valve, there is a time delay of a few seconds until the liquid refrigerant is detected by the camera. After 20 s the bypass was deactivated. It can be observed that there is also a time delay until the liquid refrigerant in the sight glass disappears completely. After approx. 15 s, the pixel value for liquid detection falls below the threshold value. The visual image evaluation allows a direct comparison with the real image. It can be seen that even after falling below the threshold value, residual liquid is still present in the sight glass for approx. 30 s. Whether this is liquid refrigerant or refrigerating machine oil can only be assumed.

A detailed picture of the selected number of white pixels is shown in Figure 5 (center). It can be seen that this is a strongly fluctuating pixel value, which can only be meaningfully evaluated by selecting the limit ± 10% and the associated hysteresis.

An additional, clearly better value for the evaluation is given by the gradient of the change of the white pixels (see figure 5 (bottom). The gradient indicates the presence of liquid refrigerant in the sight glass with extraordinary accuracy. For our evaluation routine and the assignment to corresponding error events, it was useful to use both the absolute value and the gradient for the white pixels.

A significant disadvantage of the experimental setup selected here is the formation of condensation and frost on the sight glass when the corresponding evaporation temperature is reached in interaction with ambient humid air. This effect significantly hinders the image evaluation and the use of the calibrated pixel value. For an industrial application, a condensate-free setup must be ensured here. A similar effect can be observed if the camera's light source changes significantly or shifts in position.

(A)

(B)
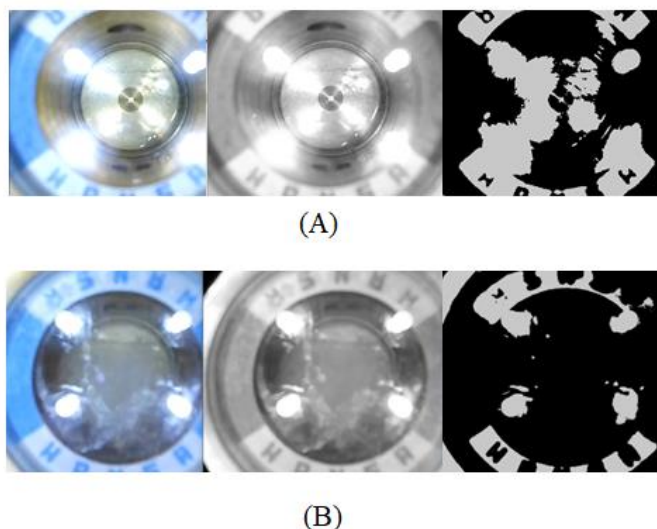
Figure 4: Sight glass with (A) pure vapor refrigerant, (B) liquid / vapor refrigerant

Measurement events

Calculated binary pixels
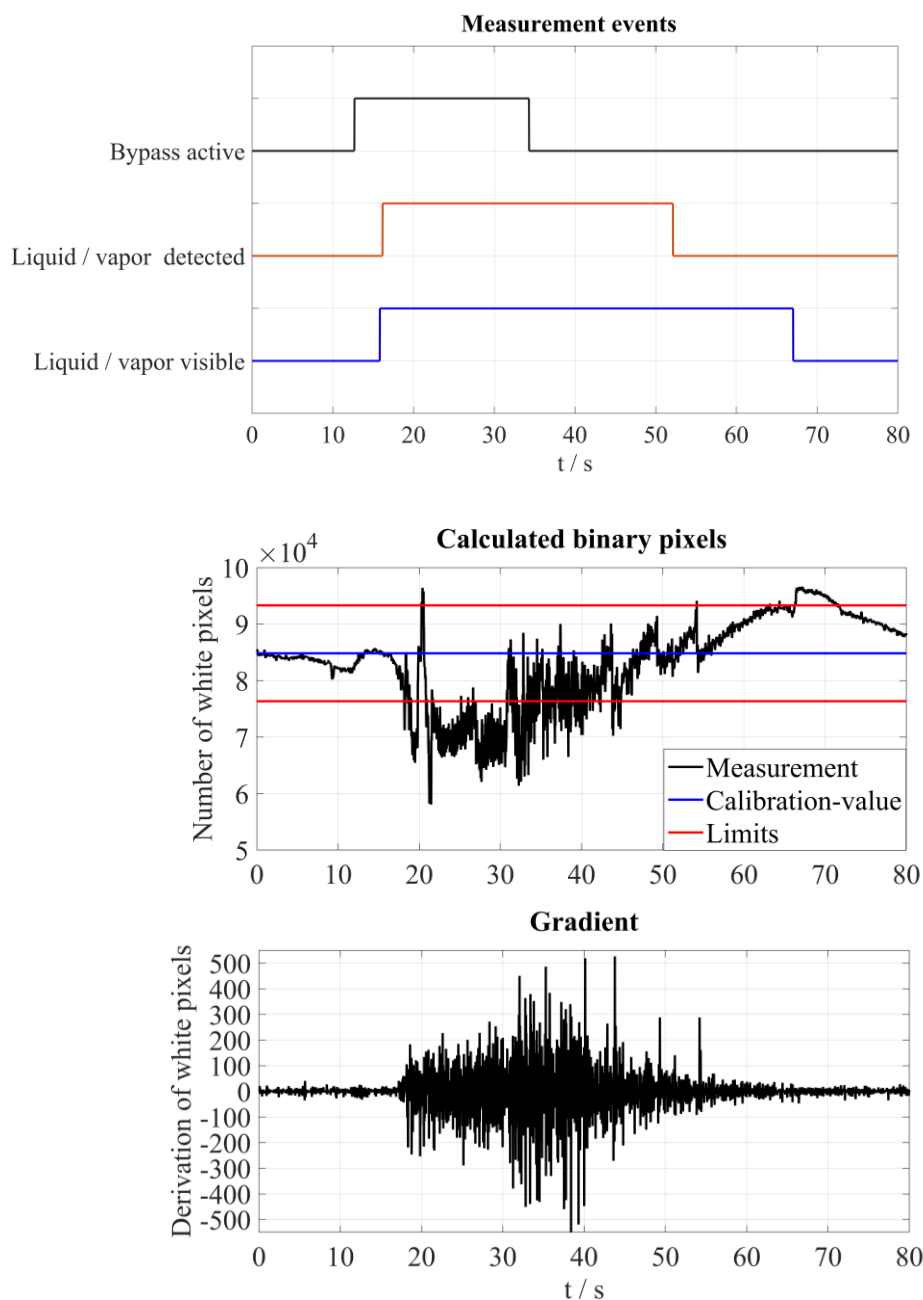

Gradient

**Figure 5:** Measurement results for image processing

3.2 Method B – Vibration Analysis on a Cantilever

3.2.1 Approach and working principle

The method describes an invasive solution approach based on the principle of vibration analysis. If a cantilever is inserted in the suction gas flow, it receives an excitation due to the operation of the system, which causes it to vibrate at its natural frequency. This system excitation is superimposed by the fluid forces of the suction gas flow. The fluid forces are proportional to velocity and density. Below the critical point, liquids in most cases have a higher density in comparison to that of the vapor. It is to be expected that in case of increasing liquid or vapor quality in the suction line of the compressor, this will have an effect on the dynamic behavior of the cantilever. By theory, this involves a damping or amplification of the amplitude of the acceleration and a shift of the natural frequency of the oscillating system.

3.2.2 Test setup
For the vibration analysis procedure as a detection method for liquid refrigerant in the suction line, a digital MEMS accelerometer type IIS2DH from ST Microelectronics was used as sensor. It was placed on the necessary circuit board orthogonal to the direction of flow. The circuit board was shaped by design like a rectangular beam and acts like a cantilever. In order to place this setup in the refrigerant flow, a pipe standard large diameter pipe section was modified accordingly as shown in Figure 7.
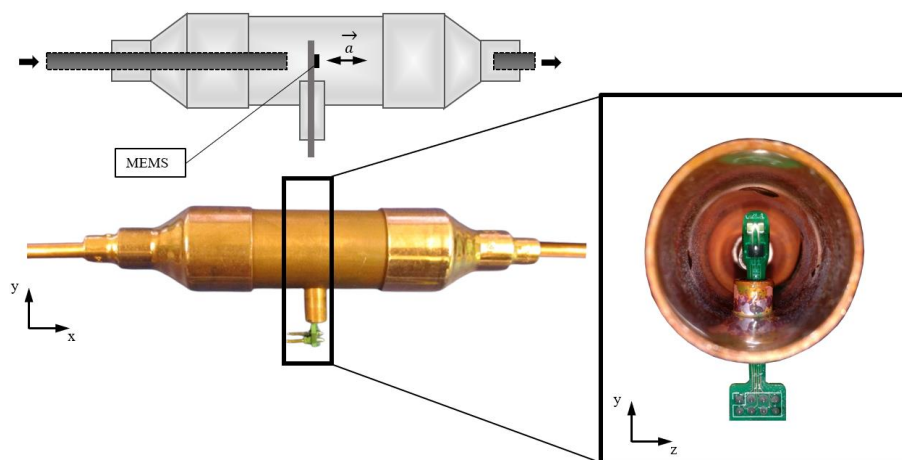
Figure 6: Modified copper tube with MEMS sensor element (left), view from inside (right),
schematic (above).

The MEMS sensor placed at the top of the cantilever detects the vibration acceleration in the direction of flow, which is caused by the system excitation and influenced by the flow forces.
Sensor configuration was realized on the software side. Both, the bandwidth and the measuring range are set to 2.667 kHz and ± 16 g. This results in a sampling frequency of 5.376 kHz and a resolution of 8 bits.
Each measurement must be started externally via the serial interface. The sensor starts to deliver digital values using an interrupt-based readout process in time steps of 0.0002 seconds (reciprocal of the sampling frequency) to a microcontroller, where they are stored internally in registers.
After the measurement, the measured values can be sent to the computer via the USB interface and evaluated there. A simultaneous data processing on microcontroller level was currently not possible due to lack of processor speed and storage limitations, but is fully realistic with adapted hardware and capable software.
The data evaluation was carried out in the time and frequency domain. For the transformation from time to frequency domain the commercial software Matlab with standard built-in functions was used.
The cost of such a MEMS accelerometer with the necessary periphery (microcontroller and sensor board) is in the range of less than 10 US$.

**3.2.3 Measurements and discussion**
At the beginning of the measurements, the test rig was operated for a sufficiently long period of time in order to achieve steady state operating conditions. The bypass was then activated again and the manually controlled expansion valve fully opened. As a result, liquid refrigerant flows through the test section (modified copper tube). The acquisition of the measurement data by the MEMS accelerometer took place 50 s before and after the switchover to bypass operation, so that the duration of the measurement is 100 s in total. The Figure 7 below shows a set of the results of the measurement in different representations.
The MEMS sensor provides the raw data as values of acceleration versus time (Fig. 8, time domain). Quantitative differences in the peak values of the acceleration during the change of the operating state of the test rig can be observed in the time signal beginning at 50 s as expected. A transfer of the data from the time domain to the frequency domain by the Fast Fourier Transformation (FFT) enables the evaluation further effects (Fig. 8, frequency domain). The FFT spectrum versus time is shown in Fig. 8, time-frequency domain. The color scale reflects the magnitude of the acceleration. The horizontal lines represent the dominant frequency components of the oscillations in the system. In the low frequency range at about 50 Hz and 108 Hz, the compressor speed and the blade pass frequency of the fan can be seen. The natural frequency of the cantilever with the MEMS sensor is around 1.5 kHz. The plot suggests only a

marginal, unrecognizable shift in the natural frequency due to the scaling of the frequency axis, but a significant damping of the amplitude can be seen. On the right side (Fig. 8, STFT) the short time Fourier transformation (STFT) is shown as a 3D-plot. Here the amplitude of the acceleration is plotted over time and frequency. A clear and recognizable damping of the vibration amplitude at the resonant frequency of the cantilever with MEMS sensor can be observed here. Other dominant frequencies due to the compressor speed remain almost unchanged.

A requirement for a suitable detection with this method is a significant natural oscillation behaviour of the sensor board with the MEMS accelerometer. Due to the high bandwidth of more than 2 kHz, a change of the frequencies in case of an event error is difficult to determine and to evaluate automatically. Another point is the magnitude of the natural frequency and the rms value of the acceleration of the cantilever in normal operation excited by the system. A well-chosen cantilever geometry will help to shift these key characteristics to reasonable values within the bandwidth of the sensor and sufficiently far away from excitation frequencies of the system.

Based on this, threshold values can be defined and relative changes can be used in the post-processing of the data. Furthermore, the choice of a suitable MEMS sensor and microcontroller for data processing is crucial for the corresponding application.
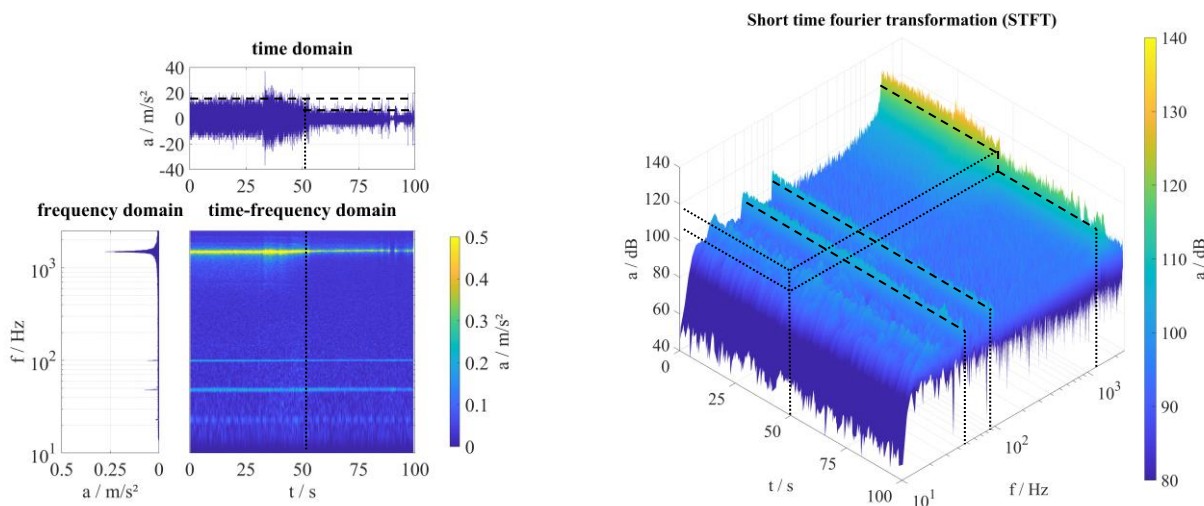
Figure 7: Acceleration signal in time and frequency domain (left), short time Fourier transformation (right).

3.3 Method C – Integral Optical Fluoroscopy

### 3.3.1 Approach and working principle
The following solution is based on the principle of different refraction coefficients and absorption of light with constant wavelength in liquid and vapor as stated by Wu et al. (2019). Therefore, the attenuation of light due to the phase change can be used as an indicator and thus as a measured variable. In case a transparent tube section is transilluminated with a light-emitting diode, the degree of absorption by tube and fluid inside can be measured by a photodiode on the corresponding opposite side. During this process, some of the light is reflected (reflection), some is absorbed (absorption), and the remaining part is transmitted (transmission) through and by the vapor liquid void fraction. In case a photodiode is connected in reverse direction with a high-impedance resistor (photoconductive mode), the current decreases with an increase in absorption of light. This results in a light-dependent voltage divider. The voltage potential between the photodiode and resistor can be used as a final quantity and recorded via a data acquisition system. If pure vapor is inside the test section, full irradiation of the photodiode is expected. If liquid components or liquid/vapor interfaces are present, the absorption/reflection increases and the measured voltage will decrease or at least change in significant quantity. It should be noted that the emitting and receiving wavelength of the diodes must be compatible with each other. Moreover, as mentioned by Wu et al. (2019), the wavelength must be selected in such a way that no reflections occur on the sight glass surfaces or that they cause excessive absorption itself.

In general, the measuring principle can be applied to determine the exact proportions of gas and liquid. However, the present analysis will only focus on the qualitative determination of liquid refrigerant being present inside the test

section. Therefore, an absolute change of the voltage in comparison to the initial state is considered. With respect to the costs, the necessary components accounted for less than 15 $.

3.3.2 Test setup

Figure 8 shows the experimental setup applied to our test rig, which consists of a light-emitting array based on eight diodes arranged in a circle, a photodiode array with similar arrangement and a microcontroller as a data acquisition system. The LED and IR photodiode arrays are attached to a both sides transparent sight glass by a 3D printed mounting. Eight LED with a wavelength of $\lambda_{LED} = 870$ nm were applied for the transmission array. The corresponding detecting array consists of eight IR photodiodes with a nominal receiving wavelength of $\lambda_{IR} = 940$ nm. For accuracy reasons, the internal A/D converter of the microcontroller was replaced by an external one, which is controlled via SPI bus. The choice of an ADC is determined by the maximum resolution and sampling frequency. Furthermore, the setup allows collecting the measured photodiode voltages at high sampling frequency ($f_s \approx 6$ kHz) on the microcontroller itself before sending them to a computer or streaming the data at low sampling frequency ($f_s \approx 700$ Hz). However, data transmission time through the serial interface has to be considered as well.
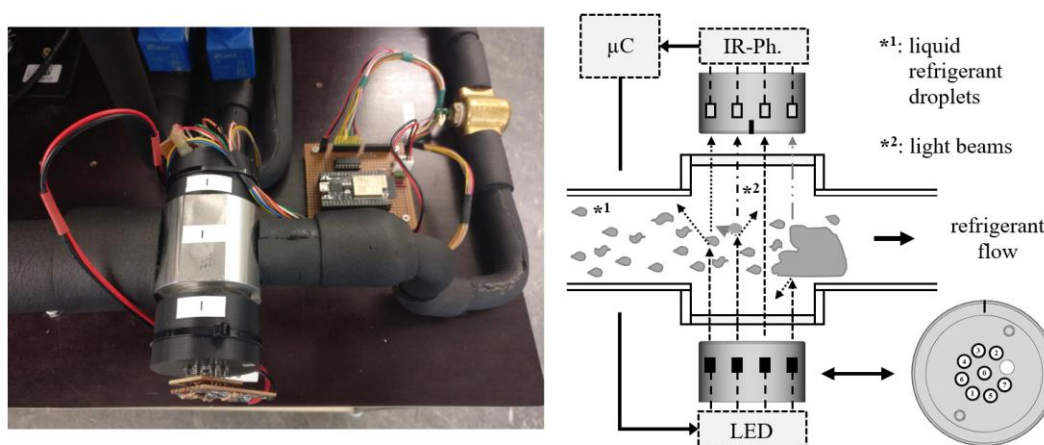
Figure 8: IR Photodiode and LED Arrays in principle (right)
and installed on the test rig (left)

For this purpose, an appropriate C++ program was written and flashed on the microcontroller. The digitally recorded values of the measuring system were later converted into a voltage value via the sensitivity of the analog-to-digital converter and analyzed using Matlab. A complete data evaluation on microcontroller level is conceivable for future application.

The transmission and detection arrays were installed at the position of sight glass B (ref. to Fig. 1). All components have been tested in preliminary tests with pure vapor as well as pure liquid inside for calibration and adjustment of the electronics, respectively.

3.3.3 Measurements and discussion

The measurement procedure is equivalent as in previous experiments. At the beginning of the measurements, the test rig was operated for a sufficiently long period of time in order to achieve steady state operating conditions. Approximately 15 s after the measurement was started, the bypass was activated for 10 seconds. Liquid refrigerant is flooding the sight glass. A small delay $\Delta t \approx 3$ s between the visual confirmation at the inspection sight glass A and the actual entry of liquid refrigerant into sight glass B is related to the downstream distance in between.

Figure 9 shows the measured voltages over time of each IR photodiode. The left vertical dotted marker line illustrates the point in time when liquid refrigerant appears to be visible inside the inspection sight glass A and therefore be present before the test section (sight glass B). Accordingly, the right vertical dotted marker line around 40 seconds represents the point in time when the initial state (pure vapor in the test section) was reached again. In case liquid refrigerant passes the test section, the attenuation of light increases. Thus, the measured voltages are decreasing depending on the position. Since the photodiodes are arranged spatially, diodes attached at the bottom of the horizontal test section (number one, five and seven) experience a higher attenuation in their signal as those mounted at the top. Due to light refraction, scattered light also may lead to interference at arbitrary photodiode positions and contribute to their voltage signal. In general, the voltage of the photodiodes decreases significantly with an increase of liquid

refrigerant in combination with liquid-vapor-interfaces inside the test section. This could be confirmed several times in subsequent measurements.

The voltage levels in the initial state or in case there is no liquid refrigerant present anymore is significantly influenced by the orientation of the transmitting and receiving unit facing each other. Hence, a fixed arrangement of LED and IR arrays is very important for reliable measurements. Formation of frost and condensation on the sight glass and hence shift of calibrated photodiode voltage levels must also be avoided. Furthermore, remaining liquid droplets or oil at the sight glass surfaces inside will make the signal noisier, even if no significant amount of liquid is present or the bypass is activated.
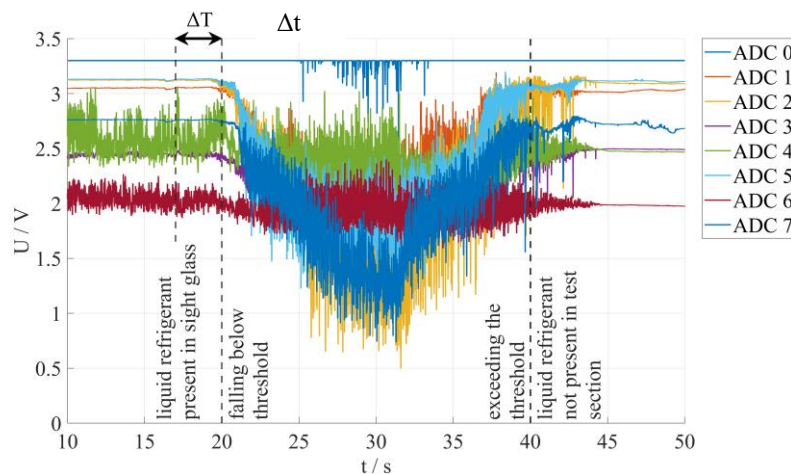
Figure 9: IR Photodiode voltages over time during measurements

4. CONCLUSIONS

The following findings could be derived from the investigations:

- All three methods were able to reliably detect quantities of liquid refrigerant within the respective test section (sight glass).
- An exact determination of the liquid (or vapor) quality is not possible with any of the methods at the present stage of development. In each case, it is the qualitative detection of liquid refrigerant to set triggers and the resulting counting of liquid refrigerant events.
- Method A – Image processing can be implemented without major effort using standard components and available libraries for image processing. The system costs are most probably highest for all three methods mainly caused by camera costs. Disadvantages are the calibration of the number of pixels at the beginning of the measurement and possible frost formation or condensation on the sight glass.
- Method B – Vibration analysis on a Cantilever is a comparatively simple and easy-to-implement solution, but it is invasive and requires a cable feedthrough from the sensor to the outside. A disadvantage is the high effort regarding data sampling, storage and time-frequency-based evaluation. An implementation to system is only possible with sufficiently good hardware.
- Method C – Integral Optical Fluoroscopy is also a comparatively simple and particularly inexpensive solution. Under certain circumstances, the use of an LED array also allows quantitative statements to be made about liquid refrigerant fraction. A disadvantage, similar to method A, is the possible formation of frost and condensation on the sight glass and hence shift of calibrated photodiode voltage levels.

NOMENCLATURE

Symbols:

f	frequency	(Hz)
f_s	sensor sampling frequency	(Hz)
a	acceleration amplitude	(m/s²), (dB)

| U | voltage | (V) |
| λ | wavelength | (nm) |

Subscripts:

MEMS	micro-electro-mechanical systems
LED	light-emitting diode
IR or IR-Ph.	infrared diode
A/D or ADC	analog to digital converter
μC	microcontroller
SPI	Serial Peripheral Interface (communication interface)
C++	programming language for the microcontroller
FFT	Fast Fourier Transformation
STFT	Short-Time Fourier Transformation

REFERENCES

Dupont, J.-L., Domanski, P., Lebrun, P., und Ziegler, F., (2019). The Role of Refrigeration in the Global Economy – 38th Informatory Note on Refrigeration Technologies. Published by the International Institute of Refrigeration. [CrossRef]

Felipe, M. A., Olegario, T., Bugtai, N., & Baldovino, R. (2019). Vision-based Liquid Level Detection in Amber Glass Bottles using OpenCV. *7th International Conference on Robot Intelligence Technology and Applications (RiTA)* (148–152). Daejeon, Korea. [CrossRef]

Gardenghi, Á. R., Filho, E. dos S., Chagas, D. G., Scagnolatto, G., Oliveira, R. M., & Tibiriçá, C. B. (2020). Overview of Void Fraction Measurement Techniques, Databases and Correlations for Two-Phase Flow in Small Diameter Channels. Fluids, 5(4), 216-242. [CrossRef]

Handoyo (2018). Gray Scale and Edge Detecting Method To Extract Raw Data in The Diffusivity Measurement System. 3rd International Seminar on Sensors, Instrumentation, Measurement and Metrology (ISSIMM) (58-60). Depok, Indonesia: IEEE. [CrossRef]

Revellin, R., Dupont, V., Ursenbacher, T., Thome, J. R., & Zun, I. (2006). Characterization of diabatic two-phase flows in microchannels: Flow parameter results for R-134a in a 0.5mm channel. International Journal of Multiphase Flow, 32(7), 755-774. [CrossRef]

Ruiz, J., Kaiser, A. S., Ballesta,M., Gil, A., & Lucas, M. (2013). Experimental measurement of cooling tower emissions using image processing of sensitive papers. Atmospheric Environment, 69, 170–181. [CrossRef]

Sarkodie, K., Fergusson-Rees, A., Makwashi, N., & Diaz, P. (2019). Slug Flow Monitoring in Pipes Using a Novel Non-Intrusive Optical Infrared Sensing Technology. SPE Europec featured at 81st EAGE Conference and Exhibition (1932-1956). London, UK: OnePetro. [CrossRef]

Sempértegui-Tapia, D., Alves, J. D. O., & Ribatski, G. (2013). Two-Phase Flow Characteristics During Convective Boiling of Halocarbon Refrigerants Inside Horizontal Small-Diameter Tubes. Heat Transfer Engineering, 34(13), 1073-1087. [CrossRef]

Wang, C., Yu, H., Zhan, N., Kang, X. & Zhang, J. (2016). A vibration probe sensor for mass flow rate measurement of gas-solid two-phase flow. Sensor Review, 36(2), 200-206. [CrossRef]

Wu, H., & Duan, Q. (2019). Gas Void Fraction Measurement of Gas-Liquid Two-Phase CO_2 Flow Using Laser Attenuation Technique. Sensors, 19(14), 3178-3191. [CrossRef]

Xiao, F., Jing, J., Han, L., Yang, L., & Wang, S. (2019). Modelling and analysis of impact forces acting on elbow in gas–liquid slug flow. Asia-Pacific Journal of Chemical Engineering, 14(2), 1-17. [CrossRef]

Zhang, J., Huang, N., Lei, L., Liang, F., Wang, X., & Wu, Z. (2020). Studies of gas-liquid two-phase flows in horizontal mini tubes using 3D reconstruction and numerical methods. International Journal of Multiphase Flow, 133. [CrossRef]

ACKNOWLEDGEMENT